EGU25-12327

U.S. NAVAL RESEARCH LABORATORY

Automated Identification of Auroral Luminosity Boundaries using pyIntensityFeatures

Angeline G. Burrell[1], Gareth Chisham[2], Nicola Longden[3], and Kate Zawdie[1]

1: Space Science Division, U.S. Naval Research Laboratory, Washington, D.C., USA; 2: British Antarctic Survey, Cambridge, UK; 3: KMPG

Abstract

Imagers that observe emissions from the atmosphere are commonly used to study various ionospheric phenomena. These phenomena include the auroral oval, equatorial plasma bubbles, and travelling ionospheric disturbances. A difficulty in using imager observations is accurately and automatically retrieving the locations of interest from these images. We present an automated method designed to identify the auroral luminosity boundaries from space-based imager data. These boundaries are important for high-latitude studies that use statistical or machine learning approaches, as geographic and magnetic coordinate systems that do not account for changes in the polar cap or equatorward auroral oval boundaries will mix together data from regions experiencing different types of coupling with the magnetosphere.

The boundary identification method was originally developed for the Imager for Magnetopause-to-Aurora Global Exploration (IMAGE) observations, and has been further adapted for use in a wider variety of situations. We will discuss the updated detection method and demonstrate the process on two different satellite data sets. The updated detection method will be made publicly accessible through a new Python package, pyIntensityFeatures.

Motivation

- The poleward and equatorward boundaries mark important physical regions.
  - Open field-lines in the polar cap.
  - Closed field lines in the auroral oval, high L-shells.
  - Closed field lines below the auroral oval, low L-shells.
- Magnetic coordinates can't accurately separate these regions, as they change based on changes in the Interplanetary Magnetic Field (IMF).
- Gridding relative to the polar cap (Open-Closed field line Boundary, OCB) and auroral oval (Equatorward Auroral Boundary, EAB) can improve space weather operations, scientific modelling, and statistical studies.
- Providing EAB and OCB locations to ionospheric models can improve our high latitude specifications and magnetospheric coupling.

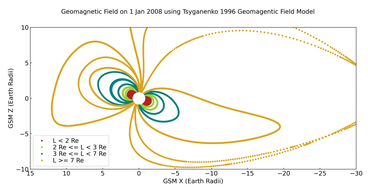

Figure 1: Tsyganenko 1996 Geomagnetic Field Model with different groups of L-shells hightlighted by color.

Background

Imagers that observe specific emission bands from the Earth's atmosphere are commonly used to study ionospheric phenomena. These phenomena include the auroral oval, equatorial plasma bubbles, and traveling ionospheric disturbances (e.g., Paxton and Meng 1999; Martinis et al. 2018; Adkins and England 2023). Images that portray the auroral oval allow for the estimation of the boundaries that mark the poleward and equatorward extents of the auroral luminosity (e.g., Shepherd et al. 1990; Longden et al. 2010), known as Auroral Luminosity Boundaries (ALBs).

The poleward ALB is often used as a proxy for the OCB (Carbary et al. 2003; Longden et al. 2010; Chisham 2017; Chisham et al. 2022), whereas the equatorward ALB is often used as a proxy for the equatorward edge of the ionosphere where the plasma flow is dominated by convection. Accurate knowledge of the boundary locations is useful for studying atmosphere-ionosphere-magnetosphere interactions during quiet and disturbed times, and is crucial for developing models and climatologies of ionospheric phenomena using adaptive co-ordinates (Redmon et al. 2010; Chisham 2017; Landry and Anderson 2018). A major difficulty in using these imager observations is the accurate and automated retrieval of locations of interest from these images, although methods have been developed in an attempt to achieve this (Longden et al. 2010; Ding et al. 2017; Chisham et al. 2022).

Decades of full and partial auroral images, from which ALBs can be calculated, currently exist in public data archives. However, databases of the boundaries themselves are more limited. *pyIntensityFeatures* provides a robust tool for creating a database of ALBs from any space-based imager (Burrell et al. 2025). These boundaries have uncertainties determined based on the quality of the identification process that allow them to be used by various statistical and machine learning methodologies.

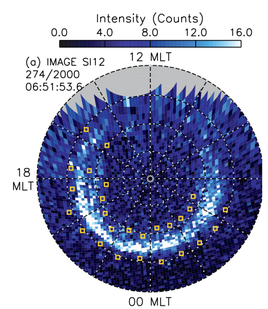

Figure 2: Figure 2(a) from Chisham et al. (2022): IMAGE SI12 intensities for 30 Sep 2000 with poleward and equatorward ALBs marked by yellow squares.

Identify features, such as auroral luminosity boundaries, in imager intensity data.

https://githubcom/aburrell/pyIntensityFeatures

For More Information

Please contact **angeline.g.burrell.civ@us.navy.mil**.

Acknowledgments

- AGB was supported by the Office of Naval Research.
- The DMSP SSUSI data is provided through CDAWeb.
- The GUVI data used here are provided through support from the NASA MO&DA program. The GUVI instrument was designed and built by The Aerospace Corporation and The Johns Hopkins University. The Principal Investigator is Dr. Larry J. Paxton.
- This poster was typeset in LaTeX.

References

Adkins, V. J. and S. L. England, 2023: Automated detection and tracking of equatorial plasma bubbles utilizing Global-Scale Observations of the Limb and Disk (GOLD) 135.6 nm data. *Earth and Space Science*, **10**, e2023EA002935, doi:10.1029/2023EA002935.

Burrell, A. G., N. S. Longden, and G. Chisham, 2025: aburrell/pyintensityfeatures: Version 0.1.0. URL `https://github.com/aburrell/pyIntensityFeatures/releases/tag/v0.1.0`

Burrell, A. G., C. van der Meeren, K. M. Laundal, and H. van Kemenade, 2024: aburrell/aacgmv2: Version 2.7.0. URL `https://github.com/aburrell/aacgmv2/tree/v2.7.0`

Carbary, J. F., T. Sotirelis, P. T. Newell, and C.-I. Meng, 2003: Auroral boundary correlations between UVI and DMSP. *Journal of Geophysical Research*, **108**, 1018, doi:10.1029/2002JA009378.

Chisham, G., 2017: A new methodology for the development of high-latitude ionospheric climatologies and empirical models. *Journal of Geophysical Research: Space Physics*, **122**, 932–947, doi:10.1002/2016JA023235.

Chisham, G., A. G. Burrell, E. G. Thomas, and Y.-J. Chen, 2022: Ionospheric boundaries derived from auroral images. **127**, e2022JA030622, doi:10.1029/2022ja030622.

Ding, G.-X., F. He, X.-X. Zhang, and B. Chen, 2017: A new auroral boundary determination algorithm based on observations from timed/guvi and dmsp/ssusi. *Journal of Geophysical Research: Space Physics*, **122**, 2162–2173, doi:10.1002/2016JA023295.

Klenzing, J., A. G. Burrell, R. Stoneback, J. Smith, L. Navarro, T. Esman, A. Govada, A. Pembroke, and C. Spence, 2024: pysat/pysatnasa: v0.0.6. URL `https://github.com/pysat/pysatNASA/releases/tag/v0.0.6`

Landry, R. G. and P. C. Anderson, 2018: An auroral boundary-oriented model of subauroral polarization streams (SAPS). *Journal of Geophysical Research: Space Physics*, **123**, 3154–3169, doi:10.1002/2017JA024921.

Longden, N., G. Chisham, M. P. Freeman, G. A. Abel, and T. Sotirelis, 2010: Estimating the location of the open-closed magnetic field line boundary from auroral images. *Annales Geophysicae*, **28**, 1659–1678, doi:10.5194/angeo-28-1659-2010.

Martinis, C., J. Baumgardner, J. Wroten, and M. Mendillo, 2018: All-sky-imaging capabilities for ionospheric space weather research using geomagnetic conjugate point observing sites. *Advances in Space Research*, **61**, 1636–1651, doi:10.1016/j.asr.2017.07.021.

Paxton, L. and C.-I. Meng, 1999: Auroral imaging/space-based optical remote sensing. *JOHNS HOPKINS APL TECHNICAL DIGEST*, **20**, 556–569.

Redmon, R. J., W. K. Peterson, L. Andersson, E. a. Kihn, W. F. Denig, M. Hairston, and R. Coley, 2010: Vertical thermal O^+ flows at 850 km in dynamic auroral boundary coordinates. *Journal of Geophysical Research*, **115**, A00J08, doi:10.1029/2010JA015589.

Shepherd, G. G., Å. Steen, and J. S. Murphree, 1990: Auroral boundary dynamics observed simultaneously from the viking spacecraft and from the ground. *Journal of Geophysical Research: Space Physics*, **95**, 5845–5865, doi:10.1029/JA095iA05p05845.

Shepherd, S. G., 2014: Altitude-adjusted corrected geomagnetic coordinates: Definition and functional approximations. *Journal of Geophysical Research: Space Physics*, **119**, 7501–7521, doi:10.1002/2014JA020264.

Methodology

The method used to identify the auroral luminosity boundaries is focused on fitting multiple Gaussian peaks with a background quadratic function to magnetic latitude (MLat) slices of intensity data measured at different magnetic local times (MLTs). Once appropriate fits are identified, the boundaries of the auroral oval can be determined by selecting the location where the fitted latitudinal profile has decreased to the desired intensity threshold. This method starts with that presented by Longden et al. (2010), which considers both single and double Gaussian fits.

The procedure to identify the ALBs may be summarized by the following steps.

1. Clean the data as directed by the instrument team.
2. Identify a scan of intensity observations that fully contain the auroral oval in one hemisphere.
3. Separate the scan into MLT slices, averaging the observed image intensities into user-specified bin sizes.
4. For each MLT slice, try to fit single, double, and triple Gaussian functions with a polynomial background.
5. Identify the poleward and equatorward boundaries at the location of a full-width at half-maximum (FWHM) away from the most poleward or equatorward Gaussian peak.
6. Evaluate each of the poleward and equatorward boundaries.
7. Select the best poleward and equatorward boundary; this may result in paired boundaries from different Gaussian fits.
8. Evaluate the MLT variation of the poleward and equatorward boundaries and remove any obvious outliers.

This methodology differs from that presented in Longden et al. (2010) in three important ways. First, it implements safeguards that allow for processing of partial auroral oval images. Second, it considers three-peaked (or more) Gaussian fits, in addition to single or double Gaussians. Third, it evaluates the consistency of the MLT variation of the boundaries across a scan. The evaluation criteria for successful Gaussian fits and boundary identifications are also adjusted based on the application to new data sets that do not fully contain the complete auroral oval in an imaging scan.

Each of the steps in the ALB identification procedure are explored in more detail for an example from the high-resolution GUVI Sensor Data Record (SDR) Lyman-Birge-Hopfield Long (LBHL) measurements. This data set is available at NASA and were obtained for this study through *pysatNASA* (Klenzing et al. 2024). The cleaning procedures applied to the data may be found there.

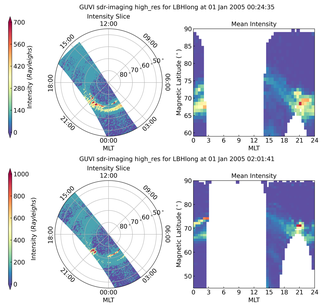

Figure 3: Northern hemisphere auroral slices of GUVI LBHL intensity observations (left) and gridded mean intensity (right) for two times with different latitude limits that were set during Step 2 of the ALB identification methodology using *pyIntensityFeatures.utils.coords.get_slice_mlat_max_min*.

Fitting the Intensity

Once an auroral slice has been compiled and averaged in latitudinal and MLT bins, fits to the latitudinal intensity profiles may be performed using *pyIntensityFeatures.utils.distributions.mult_gauss_quad*. The initial values are estimated by performing a series of simple Gaussian fits, as demonstrated in Figure 4. Once the initial values are identified, the single, double, and triple Gaussian fits with a quadratic background are obtained. Examples of the results of this fitting process for different MLT sectors are presented in Figure 6 (a), (d), (g), and (j), with that in panel (d) representing the results of the fitting to the latitudinal profile shown in Figure 4. The boundaries for each successful fit are shown in Figure 6(b), (e), (h), and (k). Figure 6(c), (f), (i), and (l) shows the final boundaries for this case with uncertainties for each boundary marked by shaded boxes. The suitability of each poleward and equatorward boundary are evaluated individually, to ensure the best boundary is selected for each location.

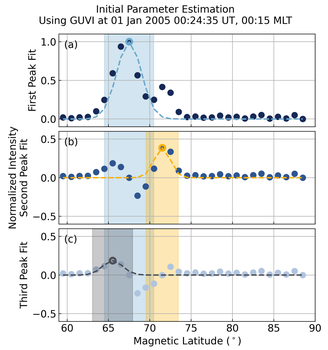

Figure 4: Identification of initial values for Gaussian fits and the maximum number of peaks allowed in a fit. Panel (a) shows the normalized latitudinal intensity profile for one MLT slice as circles. The maximum is marked with a light blue ring, and the single-peaked Gaussian fit shown using a dashed line. The FWHM distance in each direction from the peak is marked by a shaded box with the same color as the ring denoting the maximum. Panels (b) and (c) show the same process for additional peaks, for which the normalized latitudinal intensity profile has the Gaussian fit from prior peaks subtracted from it.

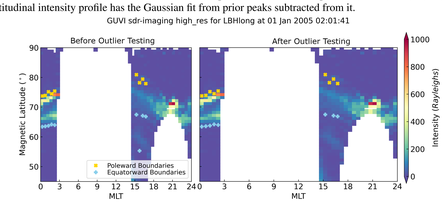

Figure 5: Successful poleward and equatorward boundaries before (right) and after (left) comparison with their MLT neighbors.

Boundary Selection

1. The boundary lies within the latitude range of the mean intensities.
2. The equatorward boundary for a given fit has a lower latitude than the poleward boundary.
3. The dayglow level is below the user-specified threshold.
4. All Gaussian parameters having appropriate signs and are in the correct hemisphere.
5. The amplitude of the Gaussian peak is at least 10% greater than the background level at its location.
6. At least one of the Gaussian peaks must have a FWHM greater than 1° latitude.
7. The primary peak should not have a FWHM greater than the width of the mean intensity grid.
8. The boundary uncertainty must be below a specified threshold (in this case 1.25°).
9. The Pearson r value is at least 0.9 and Pearson p value is no larger than 1.0×10^{-4}.

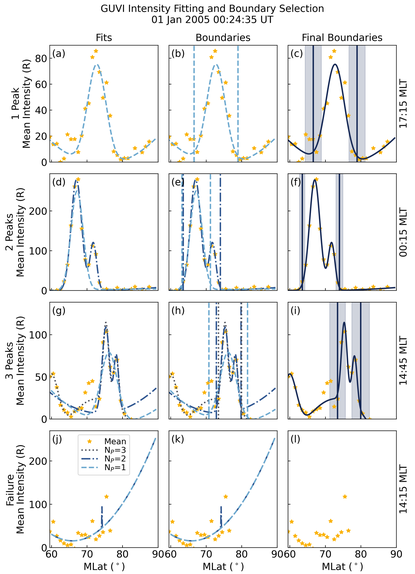

Figure 6: Gaussian fits (left; a, d, g, j), identified boundaries for each fit (middle: b, e, h, k), and selected boundaries with uncertainties along with the corresponding fit (right: c, f, i, l) for latitudinal auroral intensity profiles for MLT bins that can best be fit using a single Gaussian (top: a-c), double Gaussian (top middle: d-f), triple Gaussian (bottom middle: g-i), or for which no realistic fit is possible (bottom: j-l). The yellow stars represent the mean auroral intensity values, whereas the dashed, dot-dashed, and dotted lines show the fitted profiles and boundaries for 1, 2, and 3 Gaussian fits respectively.

If multiple ALBs pass the above criteria, the best is chosen by comparing the Pearson r and p values for each boundary and choosing the best Pearson values, with preference given to the lowest order fit.

Boundary Outlier Identification

Once obtained, the poleward and equatorward boundaries may be compared to their MLT neighbors. Figure 5 shows the boundaries from the auroral slice presented in Figure 3, with the boundaries produced by the selection process in Figure 6 shown in panel (a). Note the outlier present in the equatorward boundaries at 15:45 MLT. By calculating the running quartiles for the poleward and equatorward boundaries (with a MLT window of 5 h), this outlier can be identified and rejected. Outliers are defined as boundaries that lie more than 1.5 times the interquartile range (upper quartile - lower quartile) below the lower quartile or above the upper quartile. This yields the final set of boundaries shown in Figure 5(b). The outlier identification process can be accessed through *pyIntensityFeatures.utils.checks.evaluate_boundary_in_mlt*.